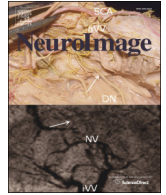




Contents lists available at ScienceDirect

NeuroImage

journal homepage: www.elsevier.com/locate/ynimg

Hippocampal sleep spindles preceding neocortical sleep onset in humans

S. Sarasso^a, P. Proserpio^b, A. Pigorini^a, F. Moroni^{c,d}, M. Ferrara^e, L. De Gennaro^c, F. De Carli^f, G. Lo Russo^b, M. Massimini^a, L. Nobili^{b,f,*}

^a Department of Biomedical and Clinical Sciences “Luigi Sacco”, Università degli Studi di Milano, 20157 Milano, Italy

^b Centre of Epilepsy Surgery “C. Munari”, Niguarda Hospital, 20162 Milano, Italy

^c Department of Psychology, “Sapienza” University of Rome, 00183 Roma, Italy

^d Department of Psychology, University of Bologna, 40126 Bologna, Italy

^e Department of Life, Health and Environmental Sciences, University of L'Aquila, 67100 L'Aquila, Italy

^f Institute of Bioimaging and Molecular Physiology, Section of Genoa, National Research Council, 16132 Genoa, Italy

ARTICLE INFO

Article history:

Accepted 17 October 2013

Available online xxxx

Keywords:

Hippocampus

Sleep spindles

Stereo-EEG

Wake-to-sleep transition

ABSTRACT

The coexistence of regionally dissociated brain activity patterns –with some brain areas being active while other already showing sleep signs– may occur throughout all vigilance states including the transition from wakefulness to sleep and may account for both physiological as well as pathological events. These dissociated electrophysiological states are often characterized by multi-domain cognitive and behavioral impairment such as amnesia for events immediately preceding sleep. By performing simultaneous intracerebral electroencephalographic recordings from hippocampal as well as from distributed neocortical sites in neurosurgical patients, we observed that sleep spindles consistently occurred in the hippocampus several minutes before sleep onset. In addition, hippocampal spindle detections consistently preceded neocortical events, with increasing delays along the cortical antero-posterior axis. Our results support the notion that wakefulness and sleep are not mutually exclusive states, but rather part of a continuum resulting from the complex interaction between diffuse neuromodulatory systems and intrinsic properties of the different thalamocortical modules. This interaction may account for the occurrence of dissociated activity across different brain structures characterizing both physiological and pathological conditions.

© 2013 Elsevier Inc. All rights reserved.

Introduction

Human sleep is considered a global phenomenon, coordinated by specialized and diffuse neuronal networks modulating the whole-brain activity. Specifically, global changes in cortical excitability associated with reduced activity of arousal/neuromodulatory systems of the reticular formation are interpreted as the main determinant of the electroencephalographic (EEG) synchronization characterizing the sleep state (Fuller et al., 2011; Moruzzi and Magoun, 1949).

However, recent evidence suggests that the coexistence of different brain states reflective of the local intrinsic properties of different corticothalamic modules may characterize both physiological and pathological sleep (Nir et al., 2011; Nobili et al., 2011; Terzaghi et al., 2012). Specifically, simultaneous intracerebral and multiunit recordings in humans revealed that most (~80%) of the Non-REM (NREM) sleep slow waves and spindles, the hallmarks of sleep state, occur locally, thus showing that some cortical regions can be active while others are silent (Nir et al., 2011). Similarly, during NREM sleep, Nobili et al.

(2011) observed brief (up to 1 min) local activations characterized by an abrupt interruption of the sleep EEG slow wave pattern in circumscribed cortical areas (primary motor cortex) replaced by a wake-like electroencephalographic high frequency pattern (alpha and/or beta rhythm). The simultaneous occurrence of heterogeneous (wake-like and sleep-like) EEG features within the sleeping brain may also underlie some common sleep disorders as confirmed by recent studies showing the presence of dysfunctional coexistence of local cortical arousal and local cortical sleep in diffuse cortical networks in patients with NREM parasomnias (Terzaghi et al., 2009, 2012).

Notably, the physiologic wake–sleep transition also seems to be characterized by the occurrence of EEG activity regulated at the regional level as suggested by scalp recordings (De Gennaro et al., 2001b; Ferrara and De Gennaro, 2011). Other groups more directly investigated the time-course of such transitions showing evidence for an asynchronous development of electrophysiological sleep features within neocortical visual areas in monkeys (Pigarev et al., 1997). More recently Magnin et al. (2010), using intracerebral EEG recordings in epileptic patients, expanded this observation to subcortical structures showing that thalamic deactivation precedes neocortical sleep onset by several minutes. Such evidence could possibly account for some of the paradoxical phenomena characterizing the wake–sleep transition (Mavromatis, 1987; Stickgold et al., 2000). Among others, several amnesic phenomena

* Corresponding author at: Centre of Epilepsy Surgery “C. Munari”, Niguarda Hospital, 20162 Milano, Italy. Fax: + 39 02 6444 2868.

E-mail address: lino.nobili@ospedaleniguarda.it (L. Nobili).

characterizing the time preceding sleep onset may be explained by a dissociation between the electrophysiological activity in the hippocampus and other brain regions. To test whether the hippocampus showed sign of sleep before neocortical regions, we employed simultaneous stereotactically implanted intracerebral (Stereo-EEG, SEEG) recordings from hippocampal as well as from several neocortical sites in nine neurosurgical patients. We then analyzed the occurrence of sleep spindles – considered, together with K-complexes, the hallmarks of NREM sleep and whose appearance is taken as evidence of the onset of sleep (De Gennaro et al., 2001a) – during the transition from wakefulness to sleep.

Materials and methods

Patients

Nine neurological patients (6M, 3F; mean age: 24; age range: 8–37) with a suspected diagnosis of drug-resistant extra-temporal focal epilepsy (i.e. the epileptogenic zone was located outside the medial temporal lobe structures) and selected as potential candidates for the surgical removal of the epileptic focus participated in the study (Table 1). During the pre-surgical assessment patients underwent individual investigation with SEEG for the precise localization of the epileptogenic zone (Cossu et al., 2005). Patients were selected based on the presence of at least two electrode contacts localized within the hippocampus. Before SEEG electrode implantation patients gave written informed consent approved by the local Ethical Committee (Niguarda Hospital, Milan, Italy). In all patients, five days after SEEG implantation, one night of sleep was recorded in order to monitor the susceptibility to seizure during sleep.

SEEG implantation procedures

Intracerebral electrodes were implanted under general anesthesia. The intra-parenchymal trajectory of these MR-compatible multilead electrodes was planned on stereo-arteriographic and 3D MR images. The procedure used was the one described by Talairach and Bancaud (1966) and later refined by Munari et al. (1994) integrated with advanced computer-aided imaging and surgical techniques (Cossu et al., 2005). The position of the intracerebral contacts (5 to 18 leads per

electrode) was ascertained by 3D MR, performed a few days after implantation.

Data recording

SEEG was recorded from platinum–iridium semiflexible multilead depth-electrodes, with a diameter of 0.8 mm, 5–18 contacts 2 mm in length and 1.5 mm intercontact distance (Dixi Medical, Besancon, France) (Cossu et al., 2005). Concurrently, scalp EEG activity was recorded from two bipolar referenced platinum needle electrodes placed during surgery at 10–20 positions Fz and Cz. Electroocular activity was recorded at the outer canthi of both eyes, and submental electromyographic activity was acquired with electrodes attached to the chin. Both EEG and SEEG signals were recorded using a 192-channel recording system (Nihon-Kohden Neurofax-110) with a sampling rate of 1000 Hz. Recordings were referenced to a contact located entirely in the white matter. Data were then exported in EEG Nihon-Kohden format and converted into MATLAB (MATLAB 7.5.0, The MathWorks Inc., Natick, MA, USA) format using customized routines. For all recorded channels, bipolar montages were calculated by subtracting the signals from adjacent contacts of the same depth-electrode to minimize common electrical noise and to maximize spatial resolution (Cash et al., 2009; Gaillard et al., 2009). Finally, data were bandpass filtered (0.3–70 Hz), using third order Butterworth filters and downsampled to 200 Hz (*resample* MATLAB routine).

For all the patients, polygraphic recordings started at lights-off. Blind to SEEG traces, one of the authors (P.P.) performed sleep scoring based on AASM criteria (Iber, 2007) applied to scalp EEG data only. We recognized SO as the first N2 sleep epoch identified by the occurrence of the first sleep spindle or K-complex recorded at the Fz–Cz scalp derivation. Spindle detection analyses were then performed on SEEG from lights-off to SO except for those patients whose SO was longer than 30 min (see Table 1). In these patients (5, 6, 8 and 9), analyses were limited to the 30 min preceding SO.

In parallel, for each patient we recorded data collected during alert wakefulness (eyes open) before lights-off (mean duration \pm SEM: 12.3 ± 1.5 min) and during the first NREM sleep episode following SO (mean duration \pm SEM: 33.6 ± 10.9 min). These data were preprocessed using the same procedures described above.

Table 1

Demographic and clinical information for each patient. R = right; L = left; F = frontal neocortex; Ins = insula; T = temporal neocortex; P = parietal neocortex; O = occipital neocortex. *SEEG assessment in this patient excluded the presence of epilepsy (for details, see Terzaghi et al., 2012). **SEEG assessment in this patient was unrevealing (no contact showed interictal/ictal signatures). The patient underwent a second SEEG investigation (not analyzed here) establishing the epileptogenic zone in the left frontal neocortex.

Patient	Gender	Age (years)	Medication (mg/day)	SEEG				SOL (min)
				Number of bipolar contacts	Hemisphere	Sample lobe	Epileptogenic zone	
1	M	8	Oxcarbazepine 600 mg/die	20	R	F, T, P	*	10
2	M	34	Levetiracetam 2000 mg/die Clonazepam 8 mg/die	13	L	F, Ins, T, P, O	Left superior temporal circonvolution	28
3	M	32	Carbamazepine 800 mg/die Phenobarbital 100 mg/die Levetiracetam 3000 mg/die	10	R	F, P	Right orbital region	15.9
4	M	37	Carbamazepine 1000 mg/die Phenytoin 300 mg/die	10	L	F, Ins, T	Left parietal operculum	14.4
5	F	34	Topiramate 500 mg/die Carbamazepine 1000 mg/die Valproate 1300 mg/die Levetiracetam 1500 mg/die	12	R	T, P, O	Right superior occipital neocortex	30
6	F	23	Carbamazepine 200 mg/die	13	L	F, Ins, P	Left frontal operculum	30
7	M	20	Carbamazepine 800 mg/die Lamotrigine 200 mg/die	35	R	F, Ins, T, P, O	Right frontal neocortex	9.3
8	M	17	Oxcarbazepine 1500 mg/die Levetiracetam 2500 mg/die	29	L	Ins, T, P, O	Left inferior temporo-occipital neocortex	30
9	F	15	Oxcarbazepine 1200 mg/die Levetiracetam 1250 mg/die	22	R	T, P, O	**	30

Bipolar contact selection

Fig. 1 and Table 1 illustrate the number and the location of the selected bipolar contacts for each patient. In brief, only SEEG bipolar contacts located in the gray matter were selected. Since we focused our investigation on sleep spindles before SO, we wanted to include only those contacts that were capable of producing sleep spindles during full-fledged NREM sleep. Thus, we further limited the number of included bipolar contacts based on the presence of visually recognizable sleep spindles during the first NREM cycle (see Fig. S1). Finally, contacts containing interictal epileptiform activity were excluded by means of visual inspection (performed by L.N.). Of note, no hippocampal contact in any patient contained epileptiform abnormalities.

SEEG spectral analysis

For each patient, spectral density analysis (Welch's averaged modified periodogram with a 4-second Hamming window) with a 0.25 Hz

bin resolution was performed on all the selected bipolar contacts. Spindle activity was calculated as the average spectral density between 11 and 16 Hz.

Detection of spindles

Spindles were detected following previously published procedures consisting of fully automatic and data-driven routines (Andrillon et al., 2011; Ferrarelli et al., 2007, 2010). Briefly, putative spindles were selected based on their power and duration. For each of the three recorded conditions (time interval between lights-off and SO, wakefulness preceding lights-off, and NREM sleep following SO) SEEG as well as scalp EEG signals were band-pass filtered between 10 and 16 Hz (-3 dB at 9.2 and 16.8 Hz) using a 2nd order Chebyshev filter. The instantaneous amplitude of the signal was computed via the Hilbert transform and two thresholds were defined based on the amplitude time-course. A detection threshold was set at mean + 3 standard deviations (SD) and amplitudes exceeding this threshold were considered potential

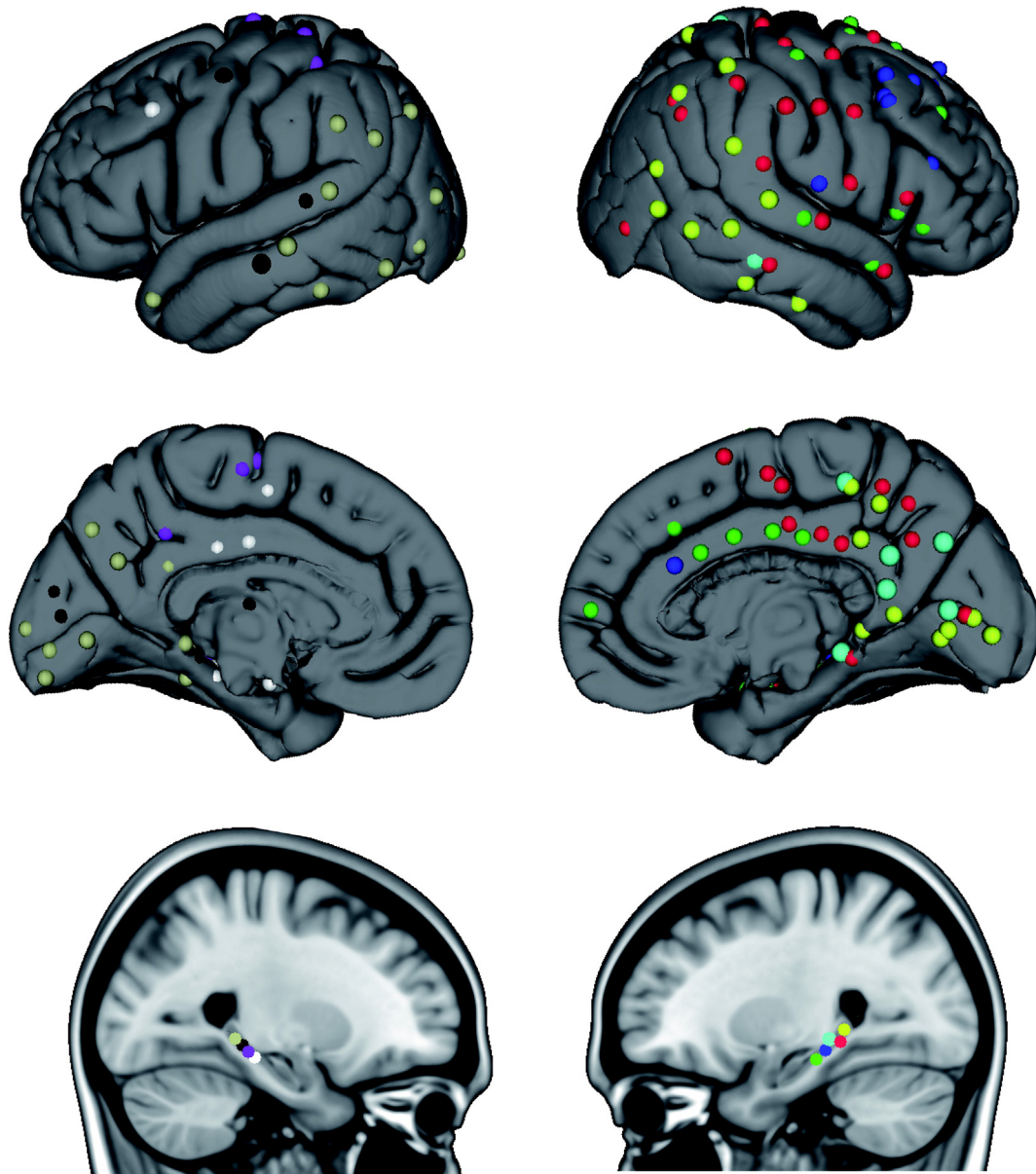


Fig. 1. Overview of the contact locations for each patient. Dots (color coded for different patients) display the selected bipolar contacts on a 3D brain reconstruction seen from lateral (top) and medial (middle) views of the two hemispheres (left on the left, right on the right). Bottom sagittal views display hippocampal bipolar contacts for each patient using the same color coding. Green, patient 1. Dark red, patient 2. Dark blue, patient 3. White, patient 4. Blue, patient 5. Violet, patient 6. Red, patient 7. Gray, patient 8. Yellow, patient 9.

spindles. A start/end threshold was set at mean + 1 SD and events whose duration was between 0.5 s and 2 s were further considered. Detections within 1 s were merged as single events. Furthermore, among these selected events, only those in which power increases were specific to the spindle range rather than broadband were considered spindles and further analyzed. In order to do so, the power of the raw EEG signal going from 1 s before the start to 1 s after the end of a detected event was computed. Only those events with the maximal power value within the spindle range (11–16 Hz) and exceeding 3SD of the average power across bins were considered real spindles and analyzed. An example of a detected sleep spindle and of the three-step procedure is provided in Fig. 2. Analyzed spindle detections were further confirmed by visual inspection performed by two of the authors (S.S. and L.N.). For each

detected event we calculated the spindle oscillation frequency calculated as the maximal power within the spindle frequency range of the spectrogram using short-time Fourier transform (± 2 s around a spindle detection, 1-second windows, 99% overlap and a resolution of 0.2 Hz; see Andrillon et al., 2011 for the use of similar procedures).

Results

Hippocampal spindles represent a sleep related phenomenon

We first assessed the presence of sleep spindles before SO by computing spindle density (number of spindles/min) calculated for different brain regions. In order to do so, for each patient we calculated the number of detected spindles per minute at any SEEG bipolar contact (Fig. 1). Then, based on their anatomical position, we merged them into different cortical areas (see Table 1) and averaged those contacts pertaining to each area across patients (Hc: hippocampus, 9 contacts; Fcx: frontal cortex, 29 contacts; Ins: insula, 7 contacts; Tcx: temporal

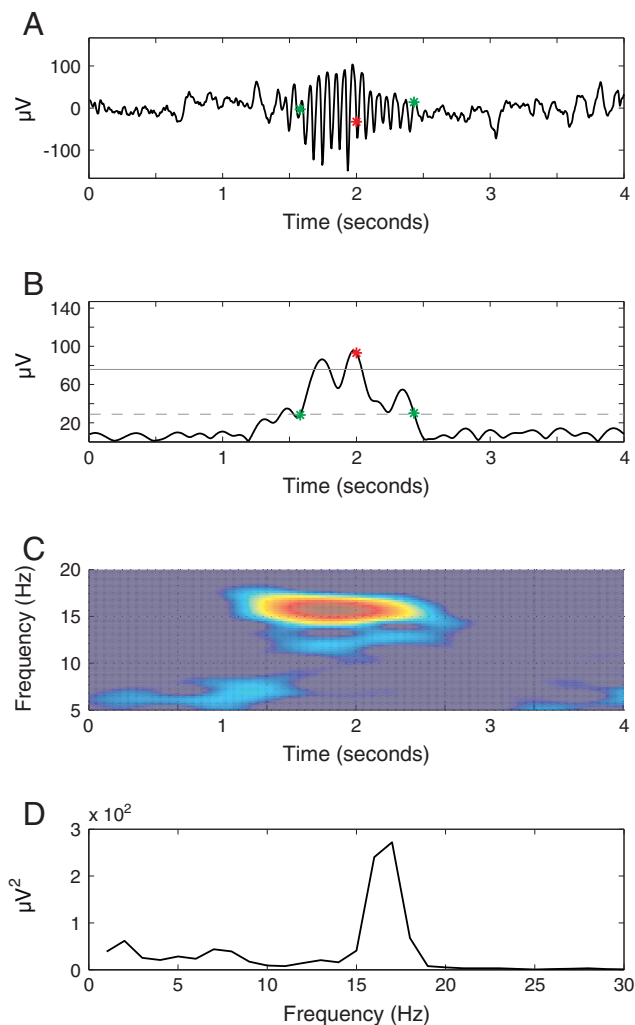


Fig. 2. Spindle detection procedure. A. Representative raw SEEG trace (4 s; filters 0.3–70 Hz) showing a spindle detected from the bipolar contact located in the hippocampus of patient 2. B. Steps one and two of the detection procedure (amplitude and duration criteria). The SEEG trace presented in A was band-pass filtered between 10 and 16 Hz (-3 dB at 9.2 and 16.8 Hz) using a 2nd order Chebyshev filter. The instantaneous amplitude of this signal was computed via the Hilbert transform (black trace). A detection threshold (solid gray line) was set at mean + 3SD and a start/end threshold (dashed gray line) was set at mean + 1SD of the amplitude during the lights-off to SO period. The green and red asterisks indicate the start/end and the center of the detected event, respectively (same in panel A). Only events crossing the detection threshold and whose duration was between 0.5 s and 2 s were further considered. C and D. Third step of the detection procedure (frequency specificity criterion). Out of the selected events, only those with the maximal power value within the spindle range (11–16 Hz) exceeding 3SD the average power across bins computed on the raw SEEG signal (from 1 s before the start to 1 s after the end of a detected event) were considered spindles and further analyzed.

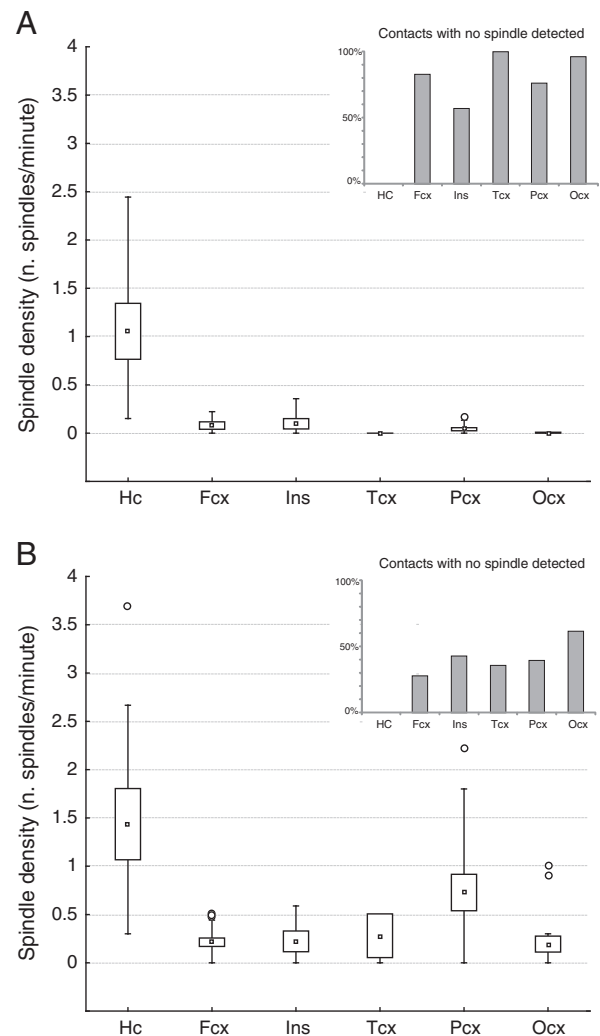


Fig. 3. Spindle density before and after SO. Spindle density across brain regions before SO (A) and during NREM sleep (B). Squares indicate the mean value, boxes indicate the SEM, whiskers indicate the non-outlier range while circles represent outliers. The two insets in A and B represent the proportion of contacts (% of the total number within each region) in which no spindle was detected before SO (A) and during NREM sleep (B). Also see Supplementary Tables 1 and 2 for a detailed description of the spindle density for individual contacts and regions. Hc: hippocampus, 9 contacts; Fcx: frontal cortex, 29 contacts; Ins: insula, 7 contacts; Tcx: temporal cortex, 14 contacts; Pcx: parietal cortex, 38 contacts; Ocx: occipital cortex, 26 contacts.

cortex, 14 contacts; Pcx: parietal cortex, 38 contacts; Ocx: occipital cortex, 26 contacts).

A One-Way ANOVA ($F_{(5,117)} = 26.34$; $p < 10^{-5}$) showed that spindle density was significantly higher in the hippocampus as compared to all the other regions (Fig. 3A; Pairwise comparison: $p < 10^{-5}$ using Bonferroni correction; mean \pm SEM Hc: 1.05 ± 0.28 spindles/min; Fcx: 0.07 ± 0.03 spindles/min; Ins: 0.09 ± 0.05 spindles/min; Pcx: 0.04 ± 0.01 spindles/min; Ocx: 0.004 ± 0.004 spindles/min). Notably, no spindle was detected in any patient and at any contact located in the neocortical temporal cortex (see Fig. 3A).

Regarding spindle oscillation frequency before SO, a One-Way ANOVA ($F_{(4,356)} = 6.21$; $p < 10^{-4}$) showed hippocampal spindles being faster than frontal and insular ones (Pairwise comparison: $p < 0.05$ using Bonferroni correction; mean \pm SEM Hc: 14.97 ± 0.06 Hz; Fcx: 14.34 ± 0.14 Hz; Ins: 13.77 ± 0.3 Hz; Pcx: 14.6 ± 0.94 Hz; Ocx: 15 ± 0.14 Hz).

Spindle detection routines applied to NREM sleep resulted in similar findings (Fig. 3B). A One-Way ANOVA ($F_{(5,117)} = 4.87$; $p < 10^{-3}$) showed higher spindle density values for hippocampus as compared to all other regions except the parietal cortex (Pairwise comparison: $p < 0.05$ using Bonferroni correction; mean \pm SEM Hc: 1.43 ± 0.36 spindles/min; Fcx: 0.21 ± 0.04 spindles/min; Ins: 0.22 ± 0.1 spindles/min; Tcx: 0.27 ± 0.22 spindles/min; Pcx: 0.72 ± 0.18 spindles/min; Ocx: 0.19 ± 0.08 spindles/min).

Similarly and in line with previous reports during NREM sleep, a One-Way ANOVA ($F_{(5,2202)} = 145.62$; $p < 10^{-5}$) applied on spindle oscillation frequency showed slower spindle frequency for frontal, insular and temporal detected events as compared to hippocampal, parietal, and occipital ones (Pairwise comparison: $p < 10^{-5}$ using Bonferroni correction; mean \pm SEM Hc: 14.61 ± 0.03 Hz; Fcx: 13.51 ± 0.04 Hz; Ins: 13.32 ± 0.07 Hz; Tcx: 13.41 ± 0.1 Hz; Pcx: 14.11 ± 0.02 Hz; Ocx: 14.83 ± 0.03 Hz).

Finally, we compared the amplitude of the hippocampal spindle events before SO with those detected during NREM sleep. Results showed that the two set of events had comparable (albeit higher during NREM) amplitude (pre-SO: 410.3 ± 97.22 μ V; NREM: 572.67 ± 119.95 μ V; Paired-Sign test: $z = 1.33$, $p = 0.18$), thus further suggesting that the hippocampal events detected during the wake–sleep transition are comparable to full-fledged sleep spindles.

On the other hand, spindle automatic detection routines applied to wake recordings preceding lights-off in all patients resulted in no false-positive detections in any of the contacts, thus suggesting that the detected events truly represent genuine sleep-related features.

Hippocampal spindles preceded neocortical spindles during the wake–sleep transition

We then calculated, for each patient and for each SEEG contact, the time interval (in minutes before SO) at which the first spindle was detected. Fig. 4A shows the overall count of detected spindles for all the bipolar contacts recorded in a representative patient (patient 2). Hippocampal spindles consistently occurred before SO in all patients (unpaired t-test; $t = 4.64$; $p < 0.005$; mean \pm SEM: 11.3 ± 2.4 min; range: 3–23 min). Also, in all patients, the occurrence of spindles in the neocortex preceded the occurrence of spindles in the hippocampus ($t = 2.75$; $p < 0.05$; mean \pm SEM: 4.5 ± 1.6 min; range: 0.15–14 min). These results were confirmed by the time course of spindle frequency power (11–16 Hz) presented in Fig. 4B. For each patient we calculated the average power density in the spindle range (11–16 Hz) over consecutive 4-second epochs at any SEEG bipolar contact between lights-off and SO. We then divided the total number of 4-second epochs for each patient in ten equally spaced deciles in order to normalize for the different durations of the lights-off to SO time interval across patients and averaged spindle power within each of them. Finally, based on the anatomical position of SEEG contacts we merged them into different cortical areas and averaged those contacts pertaining to each area across the nine patients. A One-Way ANOVA ($F_{(40,928)} = 7.85$; $p < 10^{-5}$) showed that spindle power rise significantly higher and faster ($p < 0.05$; Pairwise comparison using Bonferroni correction) over the hippocampus as compared to the other neocortical regions.

For all the patients, we then identified the first neocortical structure showing spindle detections after the hippocampus and observed that the hippocampus was consistently followed by either frontal or parietal regions. This was true for all the patients except for one (patient 6) in which spindles before SO occurred only in the hippocampus. Furthermore, we observed that, across patients, the observed hippocampus–neocortex delay for spindle occurrence was shorter in frontal and insular than in parietal areas (median frontal/insular: 1.3 min; range: 0.15–3.8 min ($n = 5$); median parietal: 10.3 min; range 5.5–14.6 min ($n = 3$); $p < 0.05$; Kolmogorov–Smirnov test).

SWA was not affected during wake–sleep transition except for frontal neocortical areas

For each patient we then calculated the change in slow wave activity (SWA; average spectral power density between 0.5 and 4 Hz) before SO at any SEEG bipolar contact. SWA reflects the occurrence and the

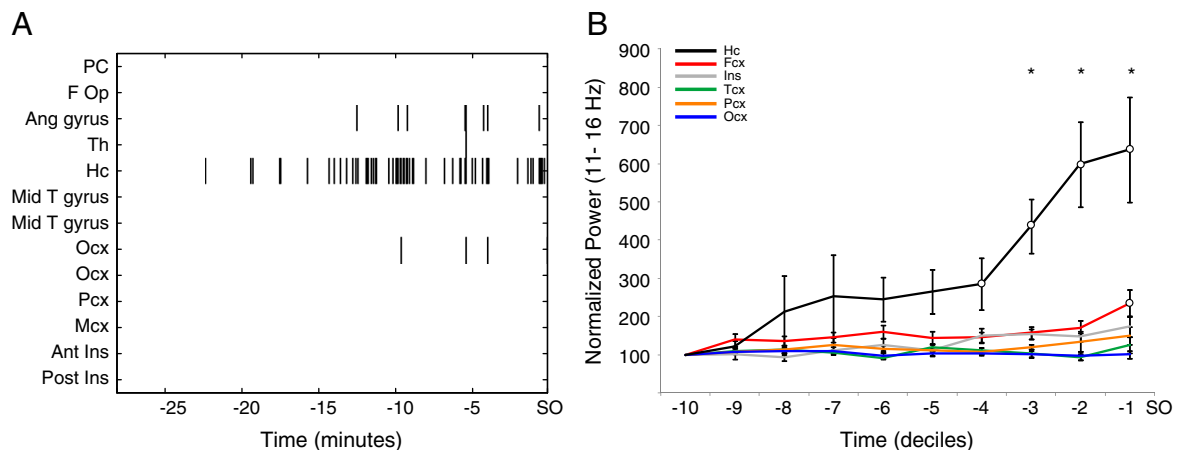


Fig. 4. Spindle activity time-course before SO. A. Spindle detection time-course before SO for a representative patient (patient 2). Rows indicate the 13 SEEG bipolar contact recorded in this patient. Black marks indicate the detection of at least one spindle in a 4-second window. PC: posterior cingulate cortex; F Op: frontal operculum; Ang gyrus: angular gyrus; Th: thalamus; Hc: hippocampus; Mid T gyrus: middle temporal gyrus; Ocx: occipital cortex; Pcx: parietal cortex; Mx: motor cortex; Ant Ins: anterior insula; Pos Ins: posterior insula. B. Spindle power time-course before SO. Error bars represent SEM. White circles indicate time-points that are significantly different from the first decile. Asterisks indicate time-points in which the hippocampus showed significant differences compared to all the other neocortical areas.

amplitude of sleep slow waves, the other EEG graphoelement that, together with sleep spindles, characterizes NREM sleep. Then, as for the spindle density analysis, SEEG contacts were merged based on their anatomical position and averaged across patients. Table 2 shows that all neocortical areas but the insula showed higher SWA at SO ($p < 0.05$) compared to the beginning of the recordings (lights-off). More importantly, only the frontal lobe showed increased SWA ($p < 0.05$) at the time of the first spindle occurring in the hippocampus. These results are in line with previously reported findings, showing a low-frequency predominance more evident over frontal scalp EEG sites during the transition from wakefulness to sleep (De Gennaro et al., 2001a, 2005).

Discussion

By exploiting SEEG recordings using data-driven, fully automatic detection algorithms to analyze the wake–sleep transition in nine neurosurgical patients, we showed that sleep spindles consistently occurred in the human hippocampus several minutes before SO. In addition, hippocampal spindle detection preceded neocortical events, with increasing delays along the cortical antero-posterior axis.

Falling asleep locally

Our results support the notion that the transition from wake to sleep is achieved through a dynamic set of events, characterized by the progressive involvement of distributed subcortical (Magnin et al., 2010) and cortical structures (Bódizs et al., 2005). This progression may be explained in terms of a diverse sensitivity of different brain regions to the reduced influence of brainstem and hypothalamic arousal promoting systems during the wake–sleep transition (Fuller et al., 2011; Saper et al., 2001). Another possibility is that this difference may reflect the influence of the homeostatic process (Borbély, 1982) over different brain structures. As such, an interesting perspective for future studies would be to confirm the present findings during prolonged wakefulness conditions, when sleep pressure is globally increased. Finally, this progression may be related to regional activity-dependent plastic changes occurring during wakefulness. As an example, a recent work showed local experience-dependent “sleep-like” EEG features occurring during wakefulness in the human cortex (Hung et al., 2013). As learning occurring during prior wakefulness affects hippocampal early sleep EEG activity (Ferrara et al., 2008), it would be interesting to investigate whether plastic changes in this region may also affect the progressive

involvement of hippocampal and neocortical areas during the transition from wake to sleep.

In line with these ideas, there is compelling evidence suggesting that frontal neocortical areas are particularly sensitive to increased homeostatic pressure, showing an especially strong response to sleep deprivation in both humans and rodents (Finelli et al., 2000; Huber et al., 2000; Marzano et al., 2010). All of the above could in principle explain why, among the investigated neocortical areas, frontal neocortical areas demonstrated shorter delays in the occurrence of sleep spindles following the hippocampus, as well as increased SWA at the time of the first hippocampal spindle occurrence during the transition from wake to sleep.

Implications for cognition and sleep medicine

The occurrence of dissociated EEG activity during the transition from wake to sleep across widespread brain regions –now including the hippocampal formation–, may also partially explain the documented occurrence of specific memory alteration or amnesia for events preceding the SO, the “mesograde amnesia” (Perlis et al., 2001; Wyatt et al., 1994, 1997). Given the central role of the hippocampal formation in episodic-declarative memory, this possibility is particularly intriguing in light of our present findings. Future studies should systematically investigate this link by looking for the detrimental effects of hippocampal spindle occurrence before and after SO on memory performance, thus shedding light on the differential impact of the pre-SO memory encoding vs the post-SO memory consolidation impairment in “mesograde amnesia”.

Our findings might be also relevant for the sleep medicine field, with important diagnostic as well as therapeutic implications. As an example, this finding may help understand the mismatch between subjective and objective SO measures frequently observed in patients with paradoxical insomnia (Manconi et al., 2010; Marzano et al., 2008; Parrino et al., 2009). On the other hand, the occurrence of dissociated activity states over widespread brain regions is in line with recent data reporting paradoxical sleep phenomena such as sleepwalking and confusional arousal, which have been attributed to a simultaneous occurrence of wakefulness and NREM sleep (Mahowald and Schenck, 2005).

Hippocampal spindles: physiologic or epileptic events?

Spindle occurrence in the human hippocampal formation and its possible relation to epileptic events is a matter of continued debate (Malow et al., 1999; Montplaisir et al., 1981; Nakabayashi et al., 2001). Solving this controversy was out of the scope of our investigation. However, our results showing reliable hippocampal spindle detections before as well as during NREM sleep were acquired during seizure-free periods in epileptic patients in which the epileptogenic zone was located outside the medial temporal lobe structures. Furthermore, the spindle detection analysis was based on data-driven and automatic detection procedures recently validated in neurosurgical epileptic patients (Andrillon et al., 2011). Finally, the absence of spindle detection during full-fledged wakefulness preceding lights-off strongly suggests that hippocampal spindles detected during the wake–sleep transition are indeed a physiologic sleep-related phenomenon rather than reflecting pathological interictal EEG activity. Supporting this view, spindles were detected in the hippocampus of patient 1, in which no interictal or ictal epileptiform abnormalities could be found at any SEEG derivation and whose clinical and SEEG assessment ruled out a diagnosis of epilepsy (Table 1; for a detailed description, see Terzaghi et al., 2012).

Hippocampal spindle origin

Regarding the origin of spindle activity recorded in the hippocampus, in one patient (patient 2) we recorded SEEG activity from one bipolar contact located in the anterior thalamic nucleus. We therefore

Table 2

SWA changes during the wake–sleep transition. For each patient we calculated the change in slow wave activity (SWA; average spectral power density between 0.5 and 4 Hz) during the wake–sleep transition for each SEEG bipolar contact. Then, based on the anatomical position of SEEG contacts we merged them into different brain regions and averaged those contacts pertaining to each region across the nine patients (Hc: hippocampus, 9 contacts; Fcx: frontal cortex, 29 contacts; Ins: insula, 7 contacts; Tcx: temporal cortex, 14 contacts; Pcx: parietal cortex, 38 contacts; Ocx: occipital cortex, 26 contacts). Specifically, for each brain region, we calculated the mean \pm SD of SWA (1) at the time of the first hippocampal spindle (average of five consecutive 4-second epochs centered on the epoch in which the spindle occurred) and (2) at SO (average of the last five consecutive 4-second epochs before SO) and expressed these values as percentage of the average SWA during the first five consecutive 4-second epochs after lights-off. t and p-values are referred to the comparisons between (1) and (2) compared to the reference value (100%) at lights-off, respectively.

Brain region	(1) SWA at first hippocampal spindle	(2) SWA at SO	t-Value		p-Value	
			(1)	(2)	(1)	(2)
Fcx	195.7 \pm 202	331.2 \pm 214	2.54	5.81	<0.05	<10 ^{−4}
Ins	120.3 \pm 60	263.9 \pm 187	0.89	2.31	n.s.	n.s.
Tcx	116.9 \pm 60	211.3 \pm 149	1.05	2.79	n.s.	<0.05
Pcx	269.1 \pm 535	373.2 \pm 566	1.94	2.97	n.s.	<0.01
Ocx	180.7 \pm 218	313.1 \pm 180	1.88	6.03	n.s.	<10 ^{−4}
Hc	129.9 \pm 57	171.2 \pm 54	1.55	3.93	n.s.	<0.01

investigated whether there was any relationship between hippocampal spindle activity and broad-band EEG thalamic activity. Together with the hippocampus, the anterior thalamic nucleus is part of the limbic system and shares reciprocal connections with the hippocampal formation via the fornix and the cingulum bundle (Aggleton et al., 2010). Although dorsal thalamic nuclei projecting to the medial temporal lobe structures are not reciprocally connected with the thalamic reticular nucleus (TRN, the spindle activity pacemaker) in cats (Jones, 2007; Paré et al., 1987; Steriade et al., 1984), the TRN was found to project to anterior thalamic nucleus in rodents (Gonzalo-Ruiz and Lieberman, 1995). It is therefore possible that the anterior thalamic nucleus, receiving TRN projections, may in turn influence hippocampal spindle activity.

Fig. S2 shows that hippocampal spindles seem to occur in phase with slow oscillations occurring in the anterior thalamic nucleus and that spindle power in this thalamic nucleus seems to be modulated concurrently. This observation is in line with the data from Magnin et al. (2010), reporting thalamic deactivation occurring several minutes before neocortical sleep onset. It is therefore possible that archicortical structures may be more sensitive to thalamic as well as brainstem and hypothalamic influences than neocortical ones, possibly following a phylogenetic determined pathway.

Concluding remarks

Overall, our results add to increasing evidence showing that wakefulness and sleep are not mutually exclusive states, but rather part of a continuum characterized by the progressive involvement of brain areas, thus allowing for the occurrence of dissociated activity patterns in different cortical and subcortical structures characterizing physiological as well as pathological conditions (Hung et al., 2013; Magnin et al., 2010; Nir et al., 2011; Nobili et al., 2011; Vyazovskiy et al., 2011; Wyatt et al., 1994, 1997).

From a methodological standpoint, our findings indicate that SEEG recordings –despite clear limitations due to the invasive nature of the technique– offer a unique opportunity to shed light on this complex brain process, allowing for a simultaneous investigation of different cortical and subcortical structures along the entire vigilance spectrum, going from active wakefulness to deep sleep. In the future, the employment of memory/cognitive paradigms coupled with this unique electrophysiological tool may foster a better understanding of the broad range of paradoxical phenomena characterizing the wake–sleep transition.

Acknowledgments

We thank Dr. Mario Rosanova and Dr. Brady A. Riedner for insightful discussions and Dr. Giovanni Casazza for statistical analysis assistance. Dr. Sarasso and Dr. Massimini gratefully acknowledge the support of “Dote ricerca”: FSE, Regione Lombardia. Dr. Moroni gratefully acknowledges a grant from the Fondazione del Monte di Bologna e Ravenna.

Conflict of interest

The authors declare no conflict of interest.

Appendix A. Supplementary data

Supplementary data to this article can be found online at <http://dx.doi.org/10.1016/j.neuroimage.2013.10.031>.

References

Aggleton, J.P., O'Mara, S.M., Vann, S.D., Wright, N.F., Tsanov, M., Erichsen, J.T., 2010. Hippocampal–anterior thalamic pathways for memory: uncovering a network of direct and indirect actions. *Eur. J. Neurosci.* 31, 2292–2307.

Andrillon, T., Nir, Y., Staba, R.J., Ferrarelli, F., Cirelli, C., Tononi, G., Fried, I., 2011. Sleep spindles in humans: insights from intracranial EEG and unit recordings. *J. Neurosci.* 31, 17821–17834.

Bódizs, R., Sverteczki, M., Lázár, A.S., Halász, P., 2005. Human parahippocampal activity: non-REM and REM elements in wake–sleep transition. *Brain Res. Bull.* 65, 169–176.

Borbély, A.A., 1982. A two process model of sleep regulation. *Hum. Neurobiol.* 1, 195–204.

Cash, S.S., Halgren, E., Deghani, N., Rossetti, A.O., Thesen, T., Wang, C., Devinsky, O., Kuzniecky, R., Doyle, W., Madsen, J.R., Bromfield, E., Eross, L., Halász, P., Karmos, G., Csercsa, R., Wittner, L., Ulbert, I., 2009. The human K-complex represents an isolated cortical down-state. *Science* 324, 1084–1087.

Cossu, M., Cardinale, F., Castana, L., Citterio, A., Francione, S., Tassi, L., Benabid, A.L., Lo Russo, G., 2005. Stereoelectroencephalography in the presurgical evaluation of focal epilepsy: a retrospective analysis of 215 procedures. *Neurosurgery* 57, 706–718 (discussion 706–718).

De Gennaro, L., Ferrara, M., Bertini, M., 2001a. The boundary between wakefulness and sleep: quantitative electroencephalographic changes during the sleep onset period. *Neuroscience* 107, 1–11.

De Gennaro, L., Ferrara, M., Curcio, G., Cristiani, R., 2001b. Antero-posterior EEG changes during the wakefulness–sleep transition. *Clin. Neurophysiol.* 112, 1901–1911.

De Gennaro, L., Vecchio, F., Ferrara, M., Curcio, G., Rossini, P.M., Babiloni, C., 2005. Antero-posterior functional coupling at sleep onset: changes as a function of increased sleep pressure. *Brain Res. Bull.* 65, 133–140.

Ferrara, M., De Gennaro, L., 2011. Going local: insights from EEG and stereo-EEG studies of the human sleep–wake cycle. *Curr. Top. Med. Chem.* 11, 2423–2437.

Ferrara, M., Iaria, G., Tempesta, D., Curcio, G., Moroni, F., Marzano, C., De Gennaro, L., Pacitti, C., 2008. Sleep to find your way: the role of sleep in the consolidation of memory for navigation in humans. *Hippocampus* 18, 844–851.

Ferrarelli, F., Huber, R., Peterson, M.J., Massimini, M., Murphy, M., Riedner, B.A., Watson, A., Bria, P., Tononi, G., 2007. Reduced sleep spindle activity in schizophrenia patients. *Am. J. Psychiatry* 164, 483–492.

Ferrarelli, F., Peterson, M.J., Sarasso, S., Riedner, B.A., Murphy, M.J., Benca, R.M., Bria, P., Kalin, N.H., Tononi, G., 2010. Thalamic dysfunction in schizophrenia suggested by whole-night deficits in slow and fast spindles. *Am. J. Psychiatry* 167, 1339–1348.

Finelli, L.A., Baumann, H., Borbély, A.A., Achermann, P., 2000. Dual electroencephalogram markers of human sleep homeostasis: correlation between theta activity in waking and slow-wave activity in sleep. *Neuroscience* 101, 523–529.

Fuller, P.M., Fuller, P., Sherman, D., Pedersen, N.P., Saper, C.B., Lu, J., 2011. Reassessment of the structural basis of the ascending arousal system. *J. Comp. Neurol.* 519, 933–956.

Gaillard, R., Dehaene, S., Adam, C., Clémenceau, S., Hasboun, D., Baulac, M., Cohen, L., Naccache, L., 2009. Converging intracranial markers of conscious access. *PLoS Biol.* 7, e61.

Gonzalo-Ruiz, A., Lieberman, A.R., 1995. Topographic organization of projections from the thalamic reticular nucleus to the anterior thalamic nuclei in the rat. *Brain Res. Bull.* 37, 17–35.

Huber, R., Deboer, T., Tobler, I., 2000. Topography of EEG dynamics after sleep deprivation in mice. *J. Neurophysiol.* 84, 1888–1893.

Hung, C.-S., Sarasso, S., Ferrarelli, F., Riedner, B., Ghilardi, M.F., Cirelli, C., Tononi, G., 2013. Local experience-dependent changes in the wake EEG after prolonged wakefulness. *Sleep* 36 (1), 59–72 (Jan 1).

Iber, C., 2007. The AASM Manual for the Scoring of Sleep and Associated Events: Rules, Terminology and Technical Specifications. American Academy of Sleep Medicine.

Jones, E.G., 2007. The Thalamus 2 Volume Set, 2nd ed. Cambridge University Press.

Magnin, M., Rey, M., Bastuji, H., Guillemand, P., Maugeyère, F., Garcia-Larrea, L., 2010. Thalamic deactivation at sleep onset precedes that of the cerebral cortex in humans. *Proc. Natl. Acad. Sci. U. S. A.* 107, 3829–3833.

Mahowald, M.W., Schenck, C.H., 2005. Insights from studying human sleep disorders. *Nature* 437, 1279–1285.

Malow, B.A., Carney, P.R., Kushwaha, R., Bowes, R.J., 1999. Hippocampal sleep spindles revisited: physiologic or epileptic activity? *Clin. Neurophysiol.* 110, 687–693.

Manconi, M., Ferri, R., Sagrada, C., Punjabi, N.M., Tettamanzi, E., Zucconi, M., Oldani, A., Castronovo, V., Ferini-Strambi, L., 2010. Measuring the error in sleep estimation in normal subjects and in patients with insomnia. *J. Sleep Res.* 19, 478–486.

Marzano, C., Ferrara, M., Sforza, E., De Gennaro, L., 2008. Quantitative electroencephalogram (EEG) in insomnia: a new window on pathophysiological mechanisms. *Curr. Pharm. Des.* 14, 3446–3455.

Marzano, C., Ferrara, M., Curcio, G., De Gennaro, L., 2010. The effects of sleep deprivation in humans: topographical electroencephalogram changes in non-rapid eye movement (NREM) sleep versus REM sleep. *J. Sleep Res.* 19, 260–268.

Mavromatis, A., 1987. Hypnagogia: The Unique State of Consciousness between Wakefulness and Sleep. Routledge.

Montplaisir, J., Leduc, L., Laverdière, M., Walsh, J., Saint-Hilaire, J.M., 1981. Sleep spindles in the human hippocampus: normal or epileptic activity? *Sleep* 4, 423–428.

Moruzzi, G., Magoun, H.W., 1949. Brain stem reticular formation and activation of the EEG. *Electroencephalogr. Clin. Neurophysiol.* 1, 455–473.

Munari, C., Hoffmann, D., Francione, S., Kahane, P., Tassi, L., Lo Russo, G., Benabid, A.L., 1994. Stereo-electroencephalography methodology: advantages and limits. *Acta Neurol. Scand. Suppl.* 152, 56–67 (discussion 68–69).

Nakabayashi, T., Uchida, S., Maehara, T., Hirai, N., Nakamura, M., Arakaki, H., Shimizu, H., Okubo, Y., 2001. Absence of sleep spindles in human medial and basal temporal lobes. *Psychiatry Clin. Neurosci.* 55, 57–65.

Nir, Y., Staba, R.J., Andrillon, T., Vyazovskiy, V.V., Cirelli, C., Fried, I., Tononi, G., 2011. Regional slow waves and spindles in human sleep. *Neuron* 70, 153–169.

Nobili, L., Ferrara, M., Moroni, F., De Gennaro, L., Russo, G.L., Campus, C., Cardinale, F., De Carli, F., 2011. Dissociated wake-like and sleep-like electro-cortical activity during sleep. *Neuroimage* 58, 612–619.

Paré, D., Steriade, M., Deschênes, M., Oakson, G., 1987. Physiological characteristics of anterior thalamic nuclei, a group devoid of inputs from reticular thalamic nucleus. *J. Neurophysiol.* 57, 1669–1685.

Parrino, L., Milioli, G., De Paolis, F., Grassi, A., Terzano, M.G., 2009. Paradoxical insomnia: the role of CAP and arousals in sleep misperception. *Sleep Med.* 10, 1139–1145.

- Perlis, M.L., Smith, M.T., Orff, H.J., Andrews, P.J., Giles, D.E., 2001. The mesograde amnesia of sleep may be attenuated in subjects with primary insomnia. *Physiol. Behav.* 74, 71–76.
- Pigarev, I.N., Nothdurft, H.C., Kastner, S., 1997. Evidence for asynchronous development of sleep in cortical areas. *Neuroreport* 8, 2557–2560.
- Saper, C.B., Chou, T.C., Scammell, T.E., 2001. The sleep switch: hypothalamic control of sleep and wakefulness. *Trends Neurosci.* 24, 726–731.
- Steriade, M., Parent, A., Hada, J., 1984. Thalamic projections of nucleus reticularis thalami of cat: a study using retrograde transport of horseradish peroxidase and fluorescent tracers. *J. Comp. Neurol.* 229, 531–547.
- Stickgold, R., Malia, A., Maguire, D., Roddenberry, D., O'Connor, M., 2000. Replaying the game: hypnagogic images in normals and amnesics. *Science* 290, 350–353.
- Talairach, J., Bancaud, J., 1966. Lesion, “irritative” zone and epileptogenic focus. *Confin. Neurol.* 27, 91–94.
- Terzaghi, M., Sartori, I., Tassi, L., Didato, G., Rustioni, V., LoRusso, G., Manni, R., Nobili, L., 2009. Evidence of dissociated arousal states during NREM parasomnia from an intracerebral neurophysiological study. *Sleep* 32, 409–412.
- Terzaghi, M., Sartori, I., Tassi, L., Rustioni, V., Proserpio, P., Lorusso, G., Manni, R., Nobili, L., 2012. Dissociated local arousal states underlying essential clinical features of non-rapid eye movement arousal parasomnia: an intracerebral stereo-electroencephalographic study. *J. Sleep Res.* 21, 502–506.
- Vyazovskiy, V.V., Olcese, U., Hanlon, E.C., Nir, Y., Cirelli, C., Tononi, G., 2011. Local sleep in awake rats. *Nature* 472, 443–447.
- Wyatt, J.K., Bootzin, R.R., Anthony, J., Bazant, S., 1994. Sleep onset is associated with retrograde and anterograde amnesia. *Sleep* 17, 502–511.
- Wyatt, J.K., Bootzin, R.R., Allen, J.J., Anthony, J.L., 1997. Mesograde amnesia during the sleep onset transition: replication and electrophysiological correlates. *Sleep* 20, 512–522.